

# Constructing thermodynamically consistent models with a non-ideal equation of state

Erkan Tüzel<sup>a,b</sup> Thomas Ihle<sup>c</sup> Daniel M. Kroll<sup>b,c</sup>

<sup>a</sup>*School of Physics and Astronomy, University of Minnesota, 116 Church Street SE, , Minneapolis, MN 55455, USA.*

<sup>b</sup>*Supercomputing Institute, University of Minnesota, 599 Walter Library, 117 Pleasant St. SE, Minneapolis, MN 55455, USA.*

<sup>c</sup>*Department of Physics, North Dakota State University, P.O. Box 5566, Fargo, ND 58102, USA.*

---

## Abstract

A recently introduced particle-based model for fluid dynamics with continuous velocities is generalized to model fluids with excluded volume effects. This is achieved through the use of biased stochastic multi-particle collisions which depend on local velocities and densities and conserve momentum and kinetic energy. The equation of state is derived and criteria for the correct choice of collision probabilities are discussed. In particular, it is shown how a naive implementation can lead to inconsistent density fluctuations.

*Key words:*

*PACS:* 47.11.+j, 05.40.+j, 02.70.Ns

---

## 1 Introduction

Simulation studies of the structure and dynamic properties of complex liquids are often complicated by the fact that typical energy scales are on the order of the thermal energy and the characteristic structural length scales are in the range of nanometers to micrometers. The resulting large number of degrees of freedom and disparate length and time scales require the use of “mesoscale” simulation techniques which achieve high computational efficiency by “averaging out” irrelevant microscopic details while retaining the essential features of the microscopic physics on the length scales of interest. The fact that the properties of these systems are strongly influenced by a delicate interplay between thermal fluctuations, hydrodynamic interactions, and possible

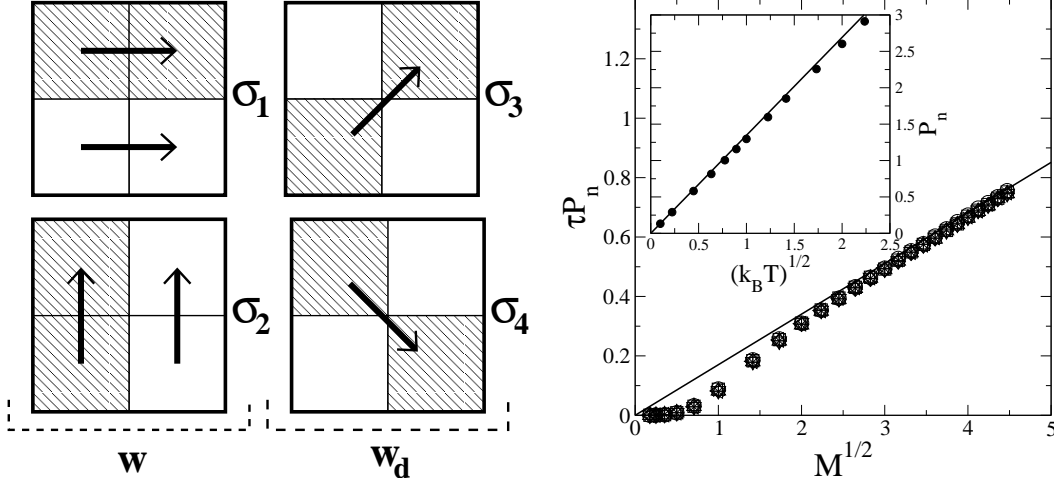


Fig. 1. Collision rules. Four distinct collisions are considered: a) horizontally along  $\sigma_1$ , b) vertically along  $\sigma_2$ , c) diagonally and d) off-diagonally along  $\sigma_3$  and  $\sigma_4$ .  $w$  and  $w_d$  denote the probabilities of choosing collisions a), b) and c), d) respectively.

Fig. 2.  $P_n$  times  $\tau$  as a function of  $M^{1/2}$ , measured using the microscopic stress tensor. Symbols show data in the range  $\tau = 0.05, \dots, 2.00$ . Parameters:  $L/a = 32$ ,  $k_B T = 1.0$ . The inset shows the nonideal contribution to the pressure as a function of  $(k_B T)^{1/2}$ . Parameters:  $L/a = 32$ ,  $M = 10$ ,  $\tau = 0.40$ . In both figures, the solid lines are the theoretical prediction given by Eq. (1).

spatio-temporally varying forces, places additional stringent requirements on the simulation protocol. A recently introduced particle-based simulation technique [1]—often called stochastic rotation dynamics (SRD) [2,3,4,5,6], multi-particle collision dynamics [7], or real-coded lattice gas [8]—is a promising algorithm for mesoscale simulations of this type. SRD solves the hydrodynamic equations of motion by following the path of fluid point-particles in discrete time and continuous space. Efficient multi-particle collisions which explicitly conserve momentum and energy enable simulations in the micro-canonical ensemble, while fully incorporating both thermal fluctuations and hydrodynamic interactions. Furthermore, its simplicity has made it possible to obtain accurate analytic expressions for the transport coefficients which are valid for both large and small mean free paths.

The original SRD algorithm—in which collisions consist of a stochastic rotation of the relative velocities of particles in the collision cells—describes a fluid with an ideal gas equation of state. The fluid is therefore very compressible, and the speed of sound,  $c_s$ , is low. However, this collision rule is not unique and other choices of collision rules can lead to nonideal behavior. In this paper we consider one such collision rule and discuss in detail the conditions which must be fulfilled in order to guarantee thermodynamic consistency. There are, however, several subtleties associated with collision rules of this type, such as phase space contraction and semi-detailed balance in this reduced phase space, which are not addressed here. In systems with

explicit interparticle potentials—such as the hard sphere fluid—this behavior can be analyzed in considerable detail. However, to the best of our knowledge, there are no non-trivial models with multi-particle interactions of the type we consider for which this has been done. The thermodynamic consistency of such models is not ensured a priori, and the aim of this paper is to provide guidelines for the construction of consistent models and to point out possible pitfalls.

A more realistic modeling of dense gases and liquids can be achieved by introducing generalized excluded volume interactions between the fluid particles. The resulting algorithm can be thought of as a coarse-grained multi-particle collision generalization of a hard sphere fluid, since, just as for hard spheres, the kinetic energy is conserved. There is no potential energy, so that the internal energy is the same as that of an ideal gas. Thermodynamic consistency therefore requires that  $c_v = T ds/dT|_\rho = dk_B/2$ , where  $d$  is the spatial dimension. It follows that the nonideal contribution to the entropy density,  $s_n$ , can only depend on the density,  $\rho$ , so that the free energy density  $f(T, \rho) = f_{ideal}(T, \rho) + Ts_n(\rho)$ . The equation of state is therefore  $P = \rho \partial f / \partial \rho|_T - f = P_{ideal} + T[\rho \partial s_n(\rho) / \partial \rho - s_n]$ , and  $P - P_{ideal}$  is strictly proportional to the temperature  $T$ .

## 2 Model

As in the original SRD algorithm, the solvent is modeled by  $N$  of point-like particles of mass  $m$  which move in continuous space with a continuous distribution of velocities. The system is coarse-grained into  $(L/a)^d$  cells of a  $d$ -dimensional cubic lattice of linear dimension  $L$  and lattice constant  $a$ . The algorithm consists of individual streaming and collision steps. In the free-streaming step, the coordinates,  $\mathbf{r}_i(t)$ , of the solvent particles at time  $t$  are updated according to  $\mathbf{r}_i(t + \tau) = \mathbf{r}_i(t) + \tau \mathbf{v}_i(t)$ , where  $\mathbf{v}_i(t)$  is the velocity of particle  $i$  at time  $t$  and  $\tau$  is the value of the discretized time step. In order to define the collision, we introduce a second grid with sides of length  $2a$  which (in  $d = 2$ ) groups four adjacent cells into one “supercell”. For simplicity, we restricted ourselves to two dimensions, but the algorithm can be easily extended to three dimensions.

As proposed in Ref. [2], a random shift of the particle coordinates before the collision step is required to ensure Galilean invariance. All particles are therefore shifted by the *same* random vector with components in the interval  $[-a, a]$  before the collision step. Particles are then shifted back by the same amount after the collision. To initiate a collision, pairs of cells in every supercell are randomly selected. As shown in Fig. 1, three distinct choices are possible: a) horizontal ( $\boldsymbol{\sigma}_1$ ), b) vertical ( $\boldsymbol{\sigma}_2$ ), and c) diagonal collisions ( $\boldsymbol{\sigma}_3$  and  $\boldsymbol{\sigma}_4$ ).

In every cell, we define the mean particle velocity,  $\mathbf{u}_n = (1/M_n) \sum_{i=1}^{M_n} \mathbf{v}_i$ , where the sum runs over all particles,  $M_n$ , in the cell with index  $n$ . The projection of the difference of the mean velocities of the selected cell-pairs on  $\boldsymbol{\sigma}_j$ ,  $\Delta u = \boldsymbol{\sigma}_j \cdot (\mathbf{u}_1 - \mathbf{u}_2)$ , is then used to determine the probability of a collision. If  $\Delta u < 0$ , no collision will be performed. For positive  $\Delta u$ , a collision will occur with an acceptance probability which depends, in principle, on  $\Delta u$  and the number of particles in the two cells,  $M_1$  and  $M_2$ . Indeed, the choice of acceptance probability,  $p_A$ , determines both the equation of state and values of the transport coefficients, and the requirement of thermodynamic consistency imposes severe restrictions on the choice of  $p_A$ . In Ref. [9] it was shown that the choice  $p_A(M_1, M_2, \Delta u) = \Theta(\Delta u) \tanh(\Lambda)$ , with  $\Lambda = A\Delta u M_1 M_2$ , where  $\Theta$  is the unit step function and  $A$  is a (small) constant leads to an equation of state of the required form. In this paper we explore the consequences of the simpler choice  $p_A = \Theta(\Delta u)$ , which is identical to the limit  $A \rightarrow \infty$  of the model presented in Ref. [9].

The collisions should conserve the total momentum and kinetic energy of the cell-pairs participating in the collision, and in analogy to the hard-sphere liquid, they should primarily transfer the component of the momentum which is parallel to the connecting vector  $\boldsymbol{\sigma}_j$ . The rule we have chosen is to exchange the parallel component of the mean velocities of the two cells, which is equivalent to a “reflection” of the relative velocities [9]. The perpendicular component remains unchanged. Because of  $x - y$  symmetry, the probabilities for choosing cell pairs in the  $x$ - and  $y$ - directions are equal, and will be denoted by  $w$ . The probability for choosing diagonal pairs is given by  $w_d = 1 - 2w$ .  $w$  and  $w_d$  must be chosen so that the hydrodynamic equations are isotropic and do not depend on the orientation of the underlying grid. As shown in Ref. [9], this can be achieved only if  $w_d = 1/2$  and  $w = 1/4$ .

### 3 Equation of state and the structure factor

The pressure can be calculated using the method described in [9]. For  $p_A = \Theta(\Delta u)$ , one finds

$$P = P_{ideal} + P_n = \rho k_B T + (b/\tau) \sqrt{\rho k_B T} \quad (1)$$

in the limit of large  $M$ , where  $\rho = M/a^2$  is the particle density and  $b = (1/4 + 1/2\sqrt{2})/2\sqrt{\pi}$ . The first term in Eq. (1) is the ideal gas contribution and the second is the contribution from the collisions, the nonideal pressure,  $P_n$ . It can be shown that  $P_n \sim \rho^2$  in the limit of small  $M$ . Simulation results for  $P_n$  obtained by averaging the diagonal part of the microscopic stress tensor [9] were found to be in good agreement with Eq. (1), see Fig. 2. This equation

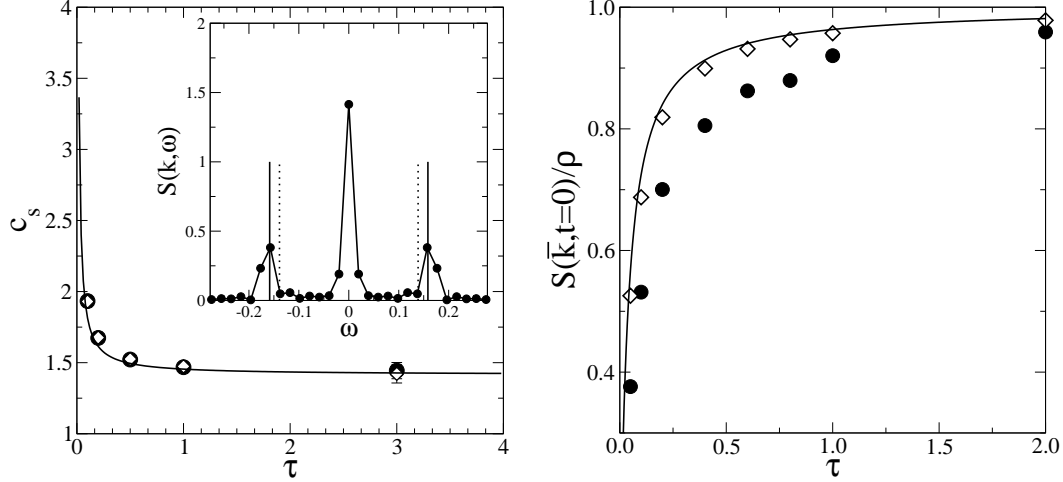


Fig. 3. Speed of sound as a function of  $\tau$ . ( $\bullet$ ) and ( $\diamond$ ) are results for  $k = (1, 0)$  and  $(0, 1)$ , respectively. The solid line is the theoretical prediction given by Eq. (2). The inset shows the dynamical structure factor as a function of  $\omega$  for  $k = (2, 0)$ ,  $\tau = 0.2$ . Parameters:  $L/a = 128$ ,  $M = 5$ ,  $k_B T = 1.0$ .

Fig. 4.  $S(\bar{k}, t = 0)/\rho$  as a function of  $\tau$  ( $\bullet$ ). ( $\diamond$ ) are results obtained by numerically evaluating the derivative of the pressure measured using the microscopic stress tensor. The solid line is a plot of Eq. (3).  $\bar{k}$  is the lowest wave vector.

of state is not consistent with the fact that the kinetic energy is conserved, since  $P - P_{ideal} \sim \sqrt{T}$  instead of  $T$ . Using Eq. (1), the adiabatic speed of sound in  $d = 2$  is

$$c_s^2 = k_B T \left[ 1 + \frac{b}{2\tau\sqrt{\rho k_B T}} \right] \left[ 2 + \frac{b}{2\tau\sqrt{\rho k_B T}} \right] . \quad (2)$$

We have performed simulations to determine the dynamical structure factor,  $S(k, \omega) = \langle \rho(k, \omega)\rho(k, \omega) \rangle$ . Measuring the structure factor can be tricky and details are discussed elsewhere.  $S(k, \omega)$  is plotted as a function of  $\omega$  in the inset to Fig. 3. The position of the finite frequency peaks in  $S(k, \omega)$  gives the speed of sound. The solid vertical lines in the figure show the theoretically predicted positions of the frequencies for the speed of sound given in Eq. (2). The dashed lines show the peak positions for an ideal gas. Results for the speed of sound for various  $k$ -values is shown in Fig. 3. The agreement with Eq. (2) is satisfactory. We have also checked that the sound speed is isotropic for the model. Thermodynamics provides a relation between density fluctuations and the derivative of the pressure; i.e. using Eq. (1),

$$S(k, t = 0) = \rho k_B T \left. \frac{\partial \rho}{\partial P} \right|_T = \frac{\rho}{1 + b/(2\tau\sqrt{\rho k_B T})} . \quad (3)$$

Fig. 4 compares simulation data for  $S(k, t = 0)/\rho$ , results for the second expression in Eq. (3) obtained by taking the numerical derivative of the measured pressure, and the analytical result, the last term in Eq. (3). Data obtained by measuring the fluctuations in the density,  $S(k, 0)$ , are clearly not consistent with the results based on measurements of the expectation value of the diagonal part of the microscopic stress tensor. As already discussed, the reason for this is that the equation of state is not consistent with the fact that the algorithm conserves kinetic energy. Note that for  $p_A = \Theta(\Delta u)$ , the collision probability does not depend on the density, which is clearly unphysical. Moreover, the presence of a  $\sqrt{\rho}$  term in Eq.(1) is strange since the first term in a typical virial expansion would be proportional to  $\rho^2$ . The consequences of choosing collision rules which violate thermodynamic consistency are therefore quite dramatic and easy to detect. However, as shown in Ref. [9], for the correct choice of collision probabilities, the algorithm can be made thermodynamically consistent.

Support from the National Science Foundation under Grant No. DMR-0513393 and ND EPSCoR through NSF grant EPS-0132289 are gratefully acknowledged. We thank A.J. Wagner for numerous discussions.

## References

- [1] A. Malevanets and R. Kapral, *J. Chem. Phys.* **110**, 8605 (1999); **112**, 7260 (2000).
- [2] T. Ihle and D.M. Kroll, *Phys. Rev. E* **63**, 020201(R) (2001); **67**, 066705 (2003); **67**, 066706 (2003).
- [3] T. Ihle, E. Tüzel, D.M. Kroll, *Phys. Rev. E* **70**, 035701(R) (2004).
- [4] E. Tüzel, M. Strauss, T. Ihle and D.M. Kroll, *Phys. Rev. E* **68**, 036701 (2003).
- [5] N. Kikuchi, C.M. Pooley, J.F. Ryder, J.M. Yeomans, *J. Chem. Phys.* **119**, 6388 (2003).
- [6] C.M. Pooley and J.M. Yeomans, *J. Phys. Chem. B* **109**, 6505 (2005).
- [7] M. Ripoll, K. Mussawisade, R.G. Winkler, and G. Gompper, *Europhys. Lett.* **68**, 106 (2004).
- [8] Y. Inoue, Y. Chen and H. Ohashi, *J. Stat. Phys.* **107**, 85 (2002).
- [9] T. Ihle, E. Tüzel, and D.M. Kroll, submitted to *Europhys. Lett.* , cond-mat/0509631.